Dalton Transactions

COMMUNICATION

View Article Online
View Journal | View Issue

Cite this: *Dalton Trans.*, 2015, **44**, 16680

Received 6th July 2015,
Accepted 23rd August 2015

DOI: 10.1039/c5dt02558c

www.rsc.org/dalton

Preferential orientations of structure directing agents in zeolites†

Eddy Dib, Antoine Gimenez, Tzonka Mineva and Bruno Alonso*

The local structure of as-synthesised silicalite-1 zeolites is modified using asymmetric $R(Pr)_3N^+$ structure directing agents. Using multi-nuclear NMR (^1H, ^{13}C, ^{14}N, ^{19}F, ^{29}Si), we show for the first time the ability of these cations to adopt preferential orientations at the zeolite channels' crossing.

The combination of interesting pore channel's topology and pore surface's functionality within crystalline solids is a key factor for the success of zeolites in a large number of fields among which are heterogeneous catalysis, adsorption and ion-exchange processes.[1–3] These textural and structural properties depend on the synthesis conditions, especially on the interplay between structure directing agents (SDA) and zeolite building units.[4,5] The design of specific SDA to reach the desired properties is therefore an important issue that still drives many research studies.

Zeolites with MFI topology (*e.g.* ZSM-5, silicalite-1, TS-1) are made of straight and sinusoidal 10 MR channels with pore diameters in the 5.0–5.5 Å range.[6] Tetrapropylammonium (TPA^+) is a well-known and efficient SDA for these zeolites.[7] It is spatially located at the crossing between the two kinds of channels (straight and sinusoidal) with each of its propyl chains pointing towards each channel direction.[8] Other tetraalkylammonium SDA have also been explored, including small symmetric[9] or asymmetric[10] molecules, *n*-alkyltrimethylammonium surfactants,[11] small diquats or triquats[9] made up of two or three ammonium groups. And recently, the use of long alkyl chain diquat surfactants has allowed the formation of layered MFI zeolites, giving rise to a significant increase in their catalytic properties by reducing the crystallite size to the nanometer range.[12]

In connection with these studies, we investigate the effect of small modifications of TPA^+ on the local structure, defined here at the scale of the zeolite crystal cell. These small modifications are a sort of chemical perturbation that may also give access to new information on the role of TPA^+ in the formation of the MFI topology. From previous ^{13}C solid-state NMR studies,[13] and notably from the different ^{13}C chemical shifts for carbons C_α and C_γ, it appears that the four propyl chains do not have the same conformation inside the as-synthesised zeolite. Therefore, one interesting approach is to replace one propyl chain by another shorter or longer chain, and to check the effect on the as-synthesised zeolite. This can give interesting insights if we are able to determine the orientation at the crossing of the channels of the asymmetric SDA: $Et(Pr)_3N^+$ (tripropylethylammonium, $TPEA^+$) and $Bu(Pr)_3N^+$ (butyltripropylammonium, $BTPA^+$). For a single molecule, it will be one of the various statistically possible orientations, or one specific and fixed orientation.

In order to look carefully at these effects, we focus on the most ordered MFI-type zeolite, the silicalite-1, formed using the fluoride route.[14] Modifications of the local order or local structure for silicalite-1 can be related to ^{13}C and ^{29}Si solid-state NMR spectrum modifications[14,15] and also to strong variations in ^{14}N quadrupolar interaction parameters as recently shown.[16]

Using this series of SDA (TPA^+, $TPEA^+$, $BTPA^+$) within a standard fluoride route procedure (see ESI 1–3†), we obtained a series of highly crystalline silicalite-1 zeolites presenting the typical crystal morphology and the X-ray diffraction patterns of MFI-type zeolites (see ESI 4 and 5†). The $^{29}Si\{^1H\}$ CP-MAS (Cross Polarization Magic Angle spinning) spectrum recorded when using TPA^+ (TPA-MFI) is typical for the silicalite-1 (Fig. 1).[15,17] By replacing TPA^+ by one of the considered asymmetric SDA, the spectrum resolution is almost preserved. We observe an upfield or downfield displacement for most of the ^{29}Si peaks, suggesting specific local modifications of the silica skeleton, probably arising from variations in SiOSi angles between the interconnected SiO_4 tetrahedrons. The explanation for these variations in ^{29}Si chemical shifts for each specific T_d site is not straightforward (see table in ESI 6†). But

Institut Charles Gerhardt Montpellier – UMR 5253 CNRS/UM/ENSCM, 8 rue de l'Ecole Normale, 34296 Montpellier Cedex 5, France. E-mail: bruno.alonso@enscm.fr; Fax: +33 4671 63470; Tel: +33 4671 63443

†Electronic supplementary information (ESI) available: Synthesis procedures, complementary solid-state multi-nuclear NMR data, SEM, XRD and TGA results. See DOI: 10.1039/c5dt02558c

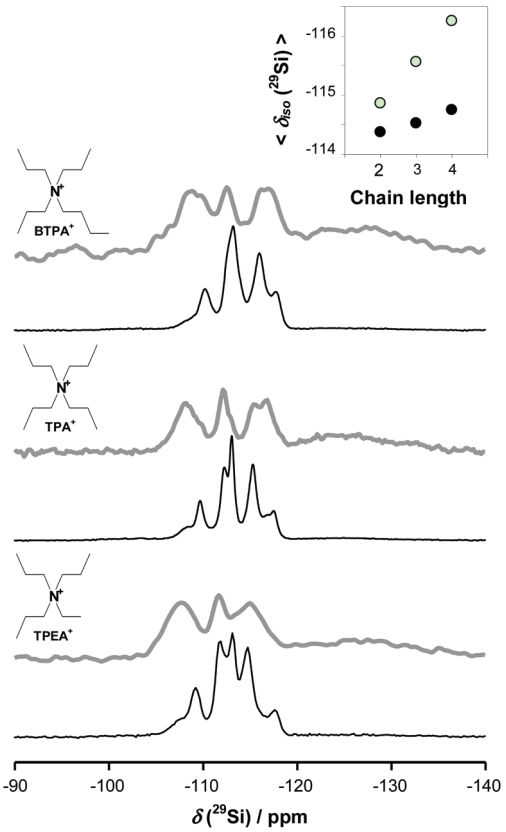

Fig. 1 $^{29}Si\{^{1}H\}$ (black) and $^{29}Si\{^{19}F\}$ (gray) NMR CP-MAS spectra of the as-synthesized zeolites (ν_0 ^{29}Si = 79.6 MHz; ν_{MAS} = 5.0 kHz). The inset presents the correlation between the length of the modified chain and the average chemical shift of the whole $^{29}Si\{^{1}H\}$ (black filled circles) and $^{29}Si\{^{19}F\}$ (clear circles) NMR CP-MAS spectra.

it is however interesting to note that these variations clearly depend on the nature of the used SDA. In addition, the average value of the ^{29}Si chemical shift varies gradually with the length of the modified alkyl group (inset in Fig. 1). These observations are confirmed when inspecting the $^{29}Si\{^{19}F\}$ CP-MAS spectra obtained with ^{19}F polarisation transfer (Fig. 1). In this case, the averaged ^{29}Si chemical shift for the T_d sites around the F^- counter anion varies even more strongly with respect to the length of the alkyl group.

The environment and location of fluorides in the silica skeleton can be explored using ^{19}F NMR. The resulting ^{19}F spectra for the three samples are very similar although not strictly identical. And the estimated chemical shift anisotropy parameters (δ_{iso}, Δ_{CSA} and η_{CSA}) for the main signal (92 to 97% in area)‡ have similar values (see ESI 6†). They are thus assigned to F^- counter-anions located in the same kind of cage $[4^15^26^2]$.[18] In these cages, F^- anions are subjected to a dynamic exchange between penta-coordinated Si sites that can be slightly affected by the geometrical variations of the silica skeleton. This may also explain the small variations observed in the ^{29}Si chemical shift of the signal corresponding to the exchange between the $SiO_{4/2}$ and $SiO_{4/2}F^-$ species (−125 ppm for TPA-MFI, −127 ppm for TPEA-MFI and for BTPA-MFI). Besides, the location of F^- anions in the same kind of cage indicates that SDA cations are probably located at the same crossing positions as the spatial distributions of both charged species are related through electrostatic interactions.[19]

^{1}H NMR MAS spectra present relatively well resolved peaks in the 0–4 ppm range assigned to the alkyl groups of the organic molecules (see ESI 6†). The very low amplitude of the well-known peak related to $SiO^-\cdots HOSi$ groups[20] (located at *ca.* 10 ppm) shows the almost lack of defects in the samples. From 2D ^{1}H–^{1}H dipolar double quantum–simple quantum correlation experiments (see ESI 6†), we conclude that each methyl or methylene CH_x group in one chain is spatially close to the other CH_x groups of the same chain, indicating that the chains are not fully extended. In the particular case of TPEA-MFI, for which the ^{1}H peaks of the two sorts of chains are more easily distinguished, the results are also consistent with the absence of close contacts between chains of different nature. This fully agrees with the location of SDA molecules at the crossing of channels with the pending chains located at the beginning of each channel, as is known for TPA^+.

In order to investigate the SDA orientations we have recorded ^{13}C solid-state NMR CP-MAS spectra (Fig. 2). In the case of TPA-MFI as-synthesised zeolites, there are two distinct signals for the C_γ(Pr) positions with a 1 : 1 signal area ratio. They are assigned to the location of the propyl chains in the two different types of channels: straight and sinusoidal ($\delta_{iso}(^{13}C)$ = 11 and 10 ppm resp.).[21] When one propyl chain is replaced by another chain, the signal area ratio between these two peaks can be: (i) preserved (1 : 1) if there is a statistical distribution of the alkyl chains within the different channels, or (ii) modified (1 : 2 or 2 : 1) if the alkyl chains have specific locations as a function of their length. Interestingly, it is this

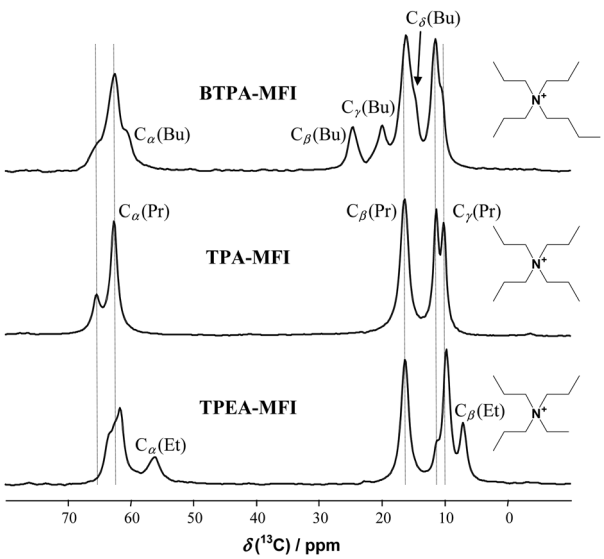

Fig. 2 $^{13}C\{^{1}H\}$ NMR CP-MAS spectra (ν_0 ^{13}C = 75.5 MHz; ν_{MAS} = 5.0 kHz).

latter case that occurred here. This means that each asymmetric tetraalkylammonium cation has a specific orientation at the crossing between the zeolite's channels. Moreover, we clearly observe an influence of the length of the alkyl chain. When a propyl chain is replaced by a smaller ethyl chain (TPEA-MFI) the signal of C_γ(Pr) in the straight channel is decreased, and this is explained by the location of the ethyl chain in this type of channel. On the contrary, in the case of BTPA-MFI, the signal of C_γ(Pr) in the sinusoidal channel is decreased, and the butyl chain is thought to be located in this other type of channel.

If we now consider the signals for the C_α(Pr) positions, there are two signals in a 1 : 3 ratio for TPA-MFI. Here, the chemical shifts' differences cannot be easily explained by the effect of the channel's nature (straight or sinusoidal), but possibly by the existence of a more distorted angular configuration for the methylene groups attached to the nitrogen (*e.g.* variations in NCC and dihedral NCCC angles) that gives rise to a signal at a higher chemical shift (65.8 ppm). The disappearance of this peak in the ^{13}C spectrum of TPEA-MFI (and not BTPA-MFI) along with the localisation of the ethyl chain in the straight channel (*vide supra*) leads us to conclude that this more distorted angular configuration corresponds to one of the propyl chains lying in the straight channel.

Additional information on the local order in zeolites can be gained from ^{14}N NMR spectroscopy. In particular, the ^{14}N quadrupolar interaction, characterised by the quadrupolar coupling constant C_Q and the quadrupolar asymmetry parameter η_Q, is very sensitive to conformational changes around the N (CNC angle distribution) as well as to the mobility[22] and to the spatial distribution of the charges (cations and counter anions).[23,24] The ^{14}N NMR spectra of the as-synthesized zeolites (Fig. 3) show similar extents for the spinning sideband (SSB) patterns. This means that the intensity of quadrupolar interactions is similar, and indeed we found C_Q values in the range 50–55 kHz by spectrum modelling (see ESI 6†). These values are different from those obtained in the case of the synthesized SDA bromide salts themselves (see ESI 6†). For this series of zeolites, the similarity between the electric field gradients at N atoms measured by ^{14}N NMR comes from a rough invariability of the three factors previously identified.[21–23] Indeed, we have shown here the preserved location of F^- counter anions in the $[4^15^26^2]$ cages (*vide supra*). And we hypothesise that CNC angle distributions are not dramatically affected by the use of asymmetric $R(Pr)_3N^+$ cations, although some different hindered vibrations may exist and could explain the slightly different ^{14}N NMR SSB envelope for BTPA-MFI.

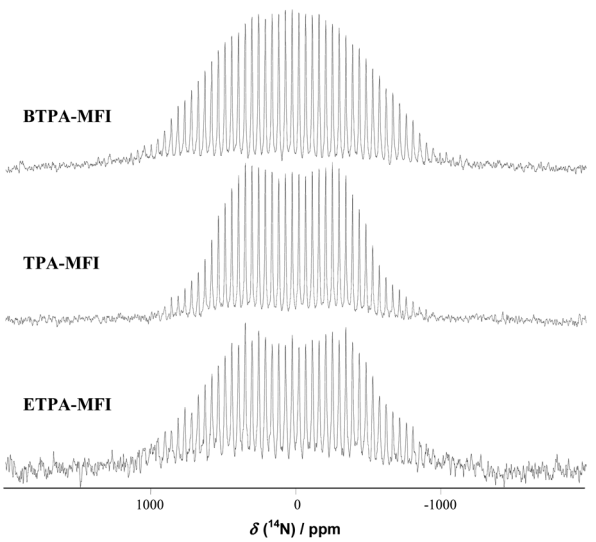

Fig. 3 ^{14}N NMR spectra of the as-synthesized zeolites ($\nu_0(^{14}N)$ = 43.3 MHz; ν_{MAS} = 2.0 kHz).

These observations, in agreement with the above presented ^{29}Si NMR data, indicate that the zeolite skeleton is able to adapt to the geometry of the organic molecule in order to reach the more stable state as a function of the intermolecular interactions (electrostatic, hydrophobic and vdW) occurring between the organic and inorganic species (SDA, silicates, F^-) during zeolite formation.

However, the flexibility of the zeolite skeleton in the presence of the asymmetric SDA does not explain why these cations adopt specific orientations at the crossing between straight and sinusoidal channels. And more precisely, why are ethyl chains occupying the straight channels, and butyl chains the sinusoidal ones? We could envisage that the main reason is a difference in steric constraints: the bulkiest chains will preferentially be located in the largest channels. But this argument is not strong enough because: (1) there are no big differences in channels' dimensions (from crystallographic data:[25] N–N distances between TPA^+ are always around 10.5 Å, and pore openings are similar); (2) this does not explain the preference of the smallest ethyl chains for a specific channel. Therefore, we think that the reason could lie in the differences in energy between conformational states. As discussed above, TPA^+ adopts a specific conformation inside ordered MFI-zeolites that leads to a characteristic ^{13}C spectrum where C_α(Pr) signals are split into two with a 1 : 3 ratio. The signal corresponding only to one C_α(Pr) atom (δ_{iso} = 65.8 ppm) is possibly the signature of an angular distortion of the propyl chain occurring at this α position. The presence of angular distortions certainly originates in the mismatch existing between the energetically preferred T_d geometry at the N site and the less symmetric geometry formed by the four channels at their crossing. Also, this distortion has an energetic cost for the system that could be reduced when the propyl chain is replaced by a shorter ethyl chain. Under these conditions, the related ^{13}C signal disappears from its specific location, as observed. On the contrary this distortion could lead to an incremented energy when the propyl chain is replaced by the butyl chain.

In the series of samples studied here, the size of the used organic molecule varies. But what will happen if we modify the organic molecule, adding for example a chemical function, while preserving its size? To answer this question, we recently synthesized EtOHTPA-MFI zeolites using $EtOHTPA^+$ (2-hydroxy-

tripopylammonium cation) as SDA (other parameters being equal). Interestingly a distribution of ^{29}Si chemical shifts is observed for the resulting silicalite-1 (see ESI 7†), but the average value of the ^{29}Si chemical shifts is the same as for TPA-MFI. This indicates clearly that there is an increase in the local disorder (also observed by the existence of a distribution in ^{14}N quadrupolar parameters) but that the average positions of the T_d sites are the same as in TPA-MFI. In other words, the zeolite skeleton did not need to adapt to a SDA of the same dimension.

Conclusions

The present study is the first demonstration that preferential orientations of the organic SDA molecules occur when asymmetric $R(Pr)_3N^+$ molecules are used in the synthesis of MFI type zeolites. In particular, ethyl chains will be located in the straight channels when using $TPEA^+$, while butyl chains will be in the sinusoidal channels when using $BTPA^+$. From multinuclear NMR data, we deduce that: (1) the spatial distribution of charges is preserved in the medium/long-range (^{14}N, ^{19}F NMR) under the effect of electrostatic interactions; (2) the zeolite silica skeleton adapts locally to the geometry of the molecule (^{29}Si NMR) so as to minimise the short-range intermolecular interaction; (3) and the SDA molecule adopts a specific orientation (^{13}C NMR) so as to minimise the conformational energy. Further work based on experimental and theoretical data is currently in progress to better define and understand the location, conformations and dynamics of these SDA.

Acknowledgements

The authors would like to thank P. Gaveau, C. Biolley and D. Laurencin for their help.

Notes and references

‡Other minor peaks are observed at around −80 ppm and −120 ppm and assigned to structure defects and residual NH_4F resp.

1 A. Corma, *Chem. Rev.*, 1997, **97**, 2373.
2 M. E. Davis, *Nature*, 2002, **417**, 813.
3 C. S. Cundy and P. A. Cox, *Chem. Rev.*, 2003, **103**, 663.
4 M. E. Davis and R. F. Lobo, *Chem. Mater.*, 1992, **4**, 756.
5 A. W. Burton, S. I. Zones and S. Elomari, *Curr. Opin. Colloid Interface Sci.*, 2005, **10**, 211.
6 D. H. Olson, G. T. Kokotailo, S. L. Lawton and W. M. Meier, *J. Phys. Chem.*, 1981, **85**, 2238.
7 C. E. Kirschhock, S. P. Kremer, P. J. Grobet, P. A. Jacobs and J. A. Martens, *J. Phys. Chem. B*, 2002, **106**, 4897.
8 H. van Koningsveld, H. van Bekkum and J. C. Jansen, *Acta Crystallogr., Sect. B: Struct. Sci.*, 1987, **43**, 127.
9 L. Beck and M. E. Davis, *Microporous Mesoporous Mater.*, 1998, **22**, 107.
10 (*a*) C. Cheng and D. Shantz, *J. Phys. Chem. B*, 2005, **109**, 13912; (*b*) S. L. Brace, P. Wormald and R. J. Darton, *Phys. Chem. Chem. Phys.*, 2015, **17**, 11950.
11 J. S. Beck, J. C. Vartuli, G. J. Kennedy, C. T. Kresge, W. J. Roth and S. E. Schramm, *Chem. Mater.*, 1994, **6**, 1816; T. Moteki, S. H. Keoh and T. Okubo, *Chem. Commun.*, 2014, **50**, 1330.
12 (*a*) M. Choi, K. Na, J. Kim, Y. Sakamoto, O. Terasaki and R. Ryoo, *Nature*, 2009, **461**, 246; (*b*) N. Kyungsu Na, J. Changbum, K. Jeongnam, C. Kanghee, J. Jung, Y. Seo, R. Messinger, B. Chmelka and R. Ryoo, *Science*, 2011, **333**, 328.
13 J. M. Chézeau, L. Delmotte, J. L. Guth and M. Soulard, *Zeolites*, 1989, **9**, 78.
14 J. L. Guth, H. Kessler and R. Wey, *Stud. Surf. Sci. Catal.*, 1986, **28**, 121.
15 J. M. Chezeau, L. Delmotte, J. L. Guth and Z. Gabelica, *Zeolites*, 1991, **11**, 598.
16 E. Dib, T. Mineva, P. Gaveau and B. Alonso, *Phys. Chem. Chem. Phys.*, 2013, **15**, 18349.
17 C. Fyfe, D. Brouwer, A. Lewis and J. M. Chézeau, *J. Am. Chem. Soc.*, 2001, **123**, 6882.
18 H. Koller, A. Wölker, L. Villaescusa, M. Díaz-Cabañas, S. Valencia and M. Camblor, *J. Am. Chem. Soc.*, 1999, **121**, 3368.
19 R. M. Shayib, N. George, R. Seshadri, A. W. Burton, S. I. Zones and B. F. Chmelka, *J. Am. Chem. Soc.*, 2011, **133**, 18728.
20 H. Koller, R. F. Lobo, S. L. Burkett and M. E. Davis, *J. Phys. Chem.*, 1995, **99**, 12588.
21 A. Abraham, R. Prins, J. van Bokhoven, E. van Eck and A. Kentgens, *Solid State Nucl. Magn. Reson.*, 2009, **35**, 61.
22 T. Mineva, P. Gaveau, A. Galarneau, D. Massiot and B. Alonso, *J. Phys. Chem. C*, 2011, **115**, 19293.
23 B. Alonso, D. Massiot, P. Florian, H. Paradies, P. Gaveau and T. Mineva, *J. Phys. Chem. B*, 2009, **113**, 11906.
24 E. Dib, B. Alonso and T. Mineva, *J. Phys. Chem. A*, 2014, **118**, 3525.
25 K. Chao, J. Lin, Y. Wang and G. H. Lee, *Zeolites*, 1986, **6**, 35.